

of the Heaviest Elements (Munksgaard, Copenhagen, 1965).

¹⁹R. L. Robinson, F. K. McGowan, P. H. Stelson, and W. T. Milner, Nucl. Phys. **A150**, 225 (1970).

²⁰O. C. Kistner and A. Scharzschild, Phys. Rev. **154**, 1182 (1966).

²¹N. K. Aras, G. D. O'Kelley, and G. Chiles, Phys. Rev. **146**, 869 (1966).

²²W. P. Pierson, Phys. Rev. **140**, B1316 (1965).

²³S. G. Nilsson, C. F. Tsang, A. Sobiczewski, Z. Szymanski, S. Wycech, C. Gustafson, I. L. Lamm, P. Möller, and B. Nilsson, Nucl. Phys. **A131**, 1 (1968).

PHYSICAL REVIEW C

VOLUME 6, NUMBER 5

NOVEMBER 1972

Neutron Resonance Spectroscopy. X. ²³²Th and ²³⁸U†

F. Rahn, H. S. Camarda,* G. Hacken, W. W. Havens, Jr., H. I. Liou, J. Rainwater, M. Slagowitz, and S. Wynchank‡

Columbia University, New York, New York 10027

(Received 21 June 1972)

Neutron time-of-flight spectroscopy measurements were made for a range of sample thicknesses of ²³²Th and ²³⁸U using the Nevis synchrocyclotron. These included transmission measurements using 200- and 40-m paths, self-indication measurements at 40 m, and Moxon-Rae capture measurements at 33 m. Resonance energies and Γ_n values were obtained for $n = 302$ levels in ²³²Th to 4.0 keV and 269 levels in ²³⁸U to 4.6 keV, with essentially no missed s levels and inclusion of a significant number of p levels. Γ_γ values were obtained for 84 levels in ²³²Th and 71 in ²³⁸U to 2400 eV, with $\langle \Gamma_\gamma \rangle = [21.2 \pm 0.3 \text{ (stat.)} \pm 0.9 \text{ (syst.)}] \text{ meV}$ (²³²Th) and $[22.9 \pm 0.5 \text{ (stat.)} \pm 0.9 \text{ (syst.)}] \text{ meV}$ (²³⁸U). In both cases a χ^2 analysis gives ~ 100 degrees of freedom including the effects of measurement errors. The values for the resonance energies were obtained from the data before the analysis was completed for Γ_n and Γ_γ values. The division of the levels into s and p populations, described in detail elsewhere, was made to achieve a "best" fit to many statistical tests relating to the orthogonal-ensemble theory for single level populations, with a resulting good fit to numerous tests. For the chosen s level population, $10^4 S_0 = (0.84 \pm 0.08)$ for ²³²Th and (1.08 ± 0.10) for ²³⁸U. The s population $\langle D \rangle = 16.7 \text{ eV}$ (²³²Th) and 20.8 eV (²³⁸U). The fits to the Porter-Thomas theory for Γ_n^0 distributions were generally good for the full 3-keV regions, with a small anomaly for the behavior of ²³²Th to 500 eV which has been reported by others. The remaining p levels have Γ_n values which are consistent with p strength function $10^4 S_1 \sim 0.9$ for ²³²Th to 400 eV and $10^4 S_1 \sim 1.4$ for ²³⁸U to 1200 eV. Larger S_1 values by other groups are due to their inclusion as stronger p levels, ones which we call s levels. Effective potential scattering radii were found to be $(9.1 \pm 0.3) \text{ fm}$ for ²³²Th and $(9.6 \pm 0.3) \text{ fm}$ for ²³⁸U.

I. INTRODUCTION

This is the tenth of a series¹ of papers reporting on our high-resolution neutron spectroscopy results using Columbia University's synchrocyclotron. The results presented in this paper were obtained during a 1970 series of measurements. Preliminary results appear in Ref. 2 for ²³²Th and Ref. 3 for ²³⁸U. The initial analysis required careful evaluation of the systematics of the results involving all the data. Our present ²³²Th and ²³⁸U data are of a far superior quality to our previous data (II) for these important elements. The isotopes ²³²Th and ²³⁸U occupy a unique place in the field of neutron cross sections and technology as potential fuel materials for use in breeder power reactors via the production of ²³³U and ²³⁹Pu. The potential useful fission energy from these materials is over two orders of magnitude greater than

from the use of ²³⁵U alone or from fossil fuels.⁴

An accurate knowledge of the neutron resonance parameters for ²³²Th and ²³⁸U is important to the fast breeder program. For this application, the energy range of interest runs to several hundred keV, with special emphasis on the s - and p -wave strength functions, level spacings, and radiation widths, for use in calculations of the cross sections in the unresolved energy regions. The breeding ratios for fast breeder reactors are greatly dependent on the average value of the total γ width $\langle \Gamma_\gamma \rangle$ and the distribution of the individual Γ_γ around the mean. Moreover the economics of nuclear power production is related to the breeding ratio which is connected to the values of the resonance parameters.

In view of their importance, the resonance parameters of ²³²Th and ²³⁸U have been measured and remeasured frequently at various laboratories as

experimental systems are improved. At the present time there are still unsatisfactorily large discrepancies between various sets of measurements. For ^{238}U , these over-all uncertainties in the design of a liquid-metal fast nuclear reactor⁵ correspond to about 3% in the evaluation of the effective multiplication factor k , 0.10 in the value of the breeding ratio, and 20% in the ^{238}U Doppler effect, which is important for safety and control considerations. Recent experimental confirmation of the applicability of the statistical orthogonal ensemble (O.E.) for the level-spacing systematics as put forth by Dyson,⁶ and Dyson and Mehta,⁷ is of interest and has implications about the fluctuations of the level spacings about their mean values, which should lead to an improved understanding of the Doppler coefficient in the unresolved energy region. A study of the statistical aspects of distributions of parameters associated with neutron resonances in nuclei in the mass region $A > 220$ is also of interest in nuclear physics. The results on the s - and p -wave strength function give further information useful in optical-model calculations, such as possible inclusion of spin-orbit coupling terms and the diffuseness of the optical potential at the nuclear surface.⁸

The values for the ^{232}Th and ^{238}U energy-level positions, with a qualitative level-strength determination was utilized before final Γ_n^0 and Γ_γ parameters were obtained. A very extensive discussion of methods for separation of such populations into s and p levels and how it was applied to ^{232}Th and ^{238}U is given by Liou, Camarda, and Rahn.⁹

The selection of which weak levels should be treated as p levels was made on the basis of many statistical tests where an attempt was made to select a total number of weak levels as s levels consistent with the Porter-Thomas theory for the Γ_n^0 distributions. We also try to have the resulting s population energy sets agree with the many statistical tests of the statistical O.E. theory for single-population level ordering. The tests include the Wigner nearest-neighbor distribution, the correlation coefficient for adjacent levels, the Dyson-Mehta Δ test for long- and short-range order in the spacing distributions, the Dyson F test, and the Bohigas and Flores $\sigma(k)$ test for the standard deviation of the spacings for levels which have k levels between them. Since a brief description of these tests is nearly impossible to make, we refer the reader to our papers for a detailed description of the theories and how our s and p selections for ^{232}Th and ^{238}U were made. The resulting s -level choices gave good agreement with all of the O.E. tests for the level-spacing distributions. The comparison of our new Γ_n^0 distributions with the Porter-Thomas theory gives generally good agreement for the energy regions to 3 keV, except for an anomaly in ^{232}Th to 500 eV. A detailed discussion of these and other results is given in Sec. IV. This includes the strength functions, S_0 and S_1 , the optical-model scattering radius, R' , and the results of various statistical tests not previously reported for the new sets of parameters.

Our new results for ^{232}Th and ^{238}U are in much better agreement with the recent studies at Sac-

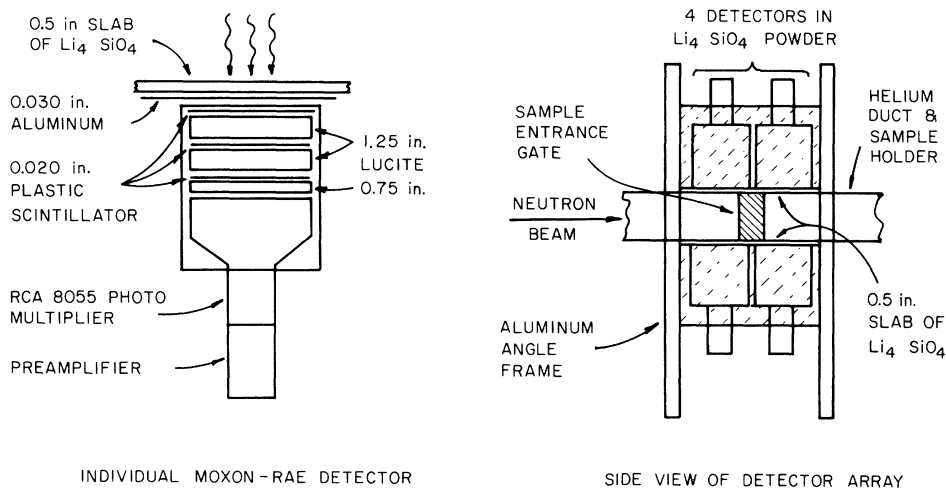


FIG. 1. The 33-m M-R detector. The collimated beam was ~ 3 in. high by 8 in. laterally while the aperture of the detector was $\sim 5 \times 12$ in. The entire flight path inside the detector was filled with He. The sample support rack of Al was not in the collimated neutron beam. Samples were typically 3×8 -in. thin foils. The sample entrance gate at the side permitted samples to be changed with little effect on the He atmosphere. The sample position is at the center of the gate in the side view.

lay,¹⁰ Harwell,^{11,12} Geel,^{13,14} and Los Alamos Scientific Laboratory (LASL) atomic bomb experiments^{15,16} than our earlier measurements. The experimental measurements of this paper represent the joint effort of all the authors. The resonance-parameter evaluations were mainly due to F. Rahn.

II. EXPERIMENTAL DETAILS

The use of the Nevis synchrocyclotron for these neutron resonance studies is essentially the same as was described in our paper VIII for the Er isotopes (1968 measurements). The 1970 measurements involved a number of system improvements. The EMR type-6050 on-line computer system used in 1968 was replaced by a type-6130 computer, and a new, more elaborate clock-interface system was used. The changes were from 8000 timing channels to 16 000 channels, from a 25- to a 20-nsec clock, and the use of a larger capacity and faster buffer storage to minimize count pile-up problems. More than 100 counts per burst were processed for "thin sample" or "open" count operation.

The collimated beam paths through the main cyclotron shield were rebuilt in a manner permitting several simultaneous measurements along other beam paths. In particular, a station at 33 m along an independent flight path was used for capture-cross-section studies using a Moxon-Rae (M-R) type detector. The data used for evaluating the resonance parameters were from 200- and 40-m "flat-detector" transmission measurements, 40-m

self-indication measurements, and the 33-m capture γ -ray detector measurements. The 200- and 40-m measurements alternately used the same flight path.

Figure 1 shows the M-R detector. It consists of an upper and lower bank of detectors, surrounded by epoxy-bonded lithium orthosilicate (Li_4SiO_4) to minimize background (n, γ) capture. The first stage of the detector, a (γ, e) converter, is also (Li_4SiO_4) which helps to shield against scattered neutrons. Calibration of the γ -ray detection efficiency per MeV of incident energy was carried out using radioisotope and capture γ sources at the Brookhaven National Laboratory High Flux Beam Reactor. The results of the calibration showed that the detection efficiency, including geometric factors, was $\sim 1.5\%$ /MeV. The M-R detector utilized a separate time-of-flight analyzer and a PDP-8 computer which was also used for various other fission time-of-flight experiments. In spite of the relatively low efficiency of the M-R detector, the counting rate was limited by the PDP-8 computer system. Our self-indication detector at 40 m had a much higher efficiency due to its use of thicker ($\frac{3}{8}$ -in.) scintillator material, and we were able to collect data at an extremely high count rate with our new higher capacity EMR-6130 computer and interface system. There was good agreement between the M-R and self-indication results. Calibrations made for the M-R detector demonstrated an accurate proportionality of the detector efficiency to γ -ray energy above 0.5 MeV with a rapid falloff in efficiency for low γ -ray en-

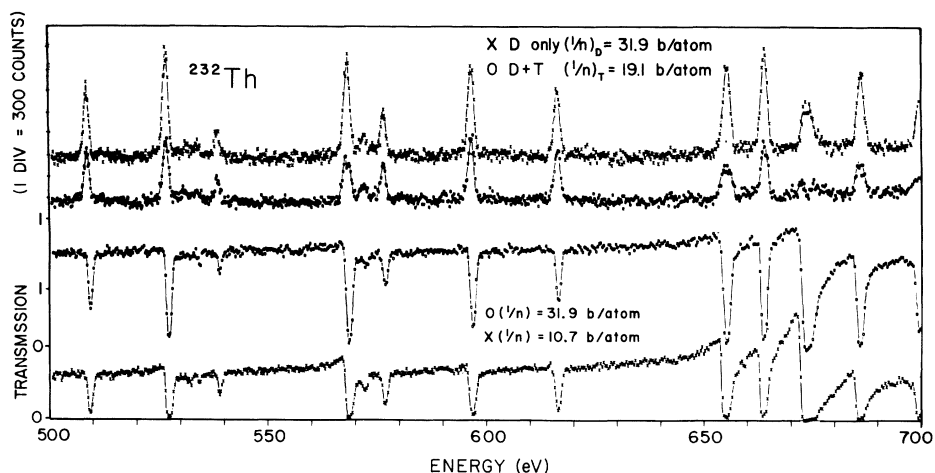


FIG. 2. Examples of the 200-m transmission and 40-m self-indication data for ^{232}Th in the energy region 500 to 700 eV. The lower part of this figure is for two of our thicker transmission samples. The thickest sample, $1/n = 10.7$ b/atom, most accurately determines the cross section between levels ($n\sigma_p \sim 1$), and tends to be black at resonance. The histogram denoted D only is self-indication data for a sample placed in the detector position at the 40-m detector. The $D+T$ histogram was obtained after adding a T sample in the beam, which reduces the size of the peaks of the D -only sample, and sometimes causes dips at the level center. The vertical scales are offset for clarity.

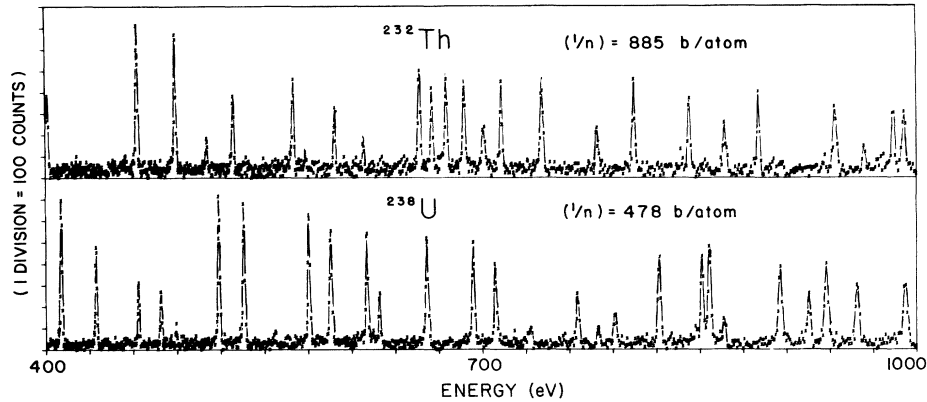


FIG. 3. Examples of the 33-m M-R data, counts versus energy from 500 to 700 eV for ^{232}Th and ^{238}U . Background has been subtracted in these plots.

ergy. This is different from that of the 40-m detector where the efficiency was nearly linear with γ energy above 1 MeV, but with a greater than proportional efficiency for the energy region from 1 to 0.4 MeV, below which there was rapidly decreasing efficiency. The agreement of the results for the two detectors from level to level suggests that the capture detection efficiency of each was essentially independent of the neutron resonance. The complex decay schemes involved in ^{232}Th and ^{238}U help in this regard.

III. DATA ANALYSIS

Natural thorium ($Z=90$) consists only of the isotope $A=232$, which has spin parity 0^+ and a half-life 1.4×10^{10} yr. Natural uranium ($Z=92$) is comprised mainly of two isotopes: $A=235$, 0.71% abundant, with spin parity $\frac{7}{2}^-$, half-life of 7.1×10^8 yr; and $A=238$, 99.3% abundant, with spin parity 0^+ , half-life 4.5×10^9 yr. All our uranium samples were depleted in ^{235}U . All the U and Th isotopes are fissionable by neutrons, but ^{232}Th and ^{238}U re-

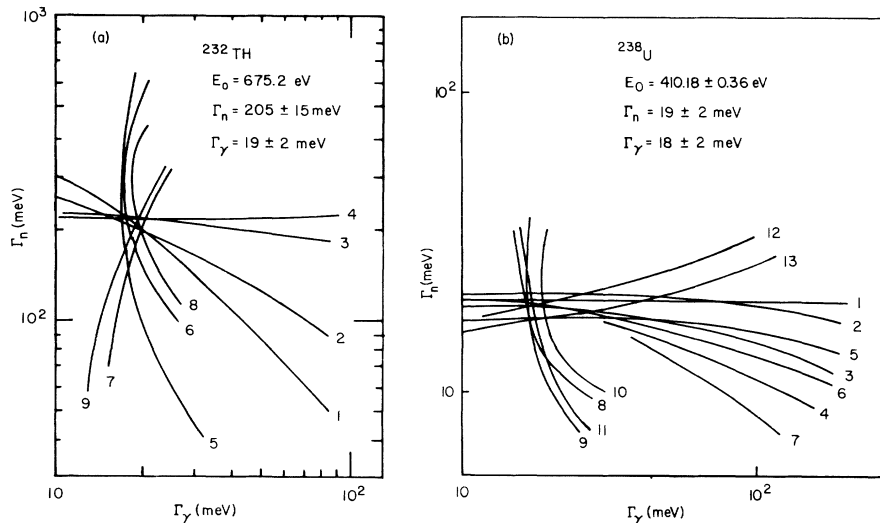


FIG. 4. Examples of the area analysis for the resonance parameters. For each level there are several curves, giving the relationship between Γ_n and Γ_γ from the transmission, self-indication, and M-R data analysis. The intersection of the curves implies the values of both Γ_n and Γ_γ in favorable cases. (a) ^{232}Th : curves 1-4 are for 200-m transmission data with $1/n = 10.7, 31.9, 191,$ and 885 b/atom, respectively; curves 5-7, for 40-m self-indication data with $1/n = 32, 191,$ and 885 b/atom; and curves 8-9, for 33-m M-R data with $1/n = 191$ and 885 b/atom. (b) ^{238}U : curves 1-4 are for 200-m transmission data with $1/n = 478, 119, 28.8,$ and 11.9 b/atom; curves 5-7, for 40-m transmission data with $1/n = 119, 27.1,$ and 8.5 b/atom; curves 8-9, for 33-m M-R data with $1/n = 119$ and 478 b/atom; curves 10-11, for D -only data with $1/n = 119$ and 478 b/atom; curves 12-13, for $D+T$ data with $R = 119/478$ and $R = 28/119$, respectively, where R is the ratio of the T sample thickness to the D -only sample thickness.

quire an incident neutron energy of greater than 1 MeV for the fission process to occur in a significant amount.

Our samples were fabricated plates $\sim 8 \times 20$ cm² in dimension, and we made measurements using inverse sample thicknesses $(1/n) = 10.7, 31.9, 36.2, 191,$ and 885 b/atom for ²³²Th and $(1/n) = 8.5, 11.9, 27.1, 28.8, 36.0, 119,$ and 478 b/atom for ²³⁸U. The thicker samples of ²³⁸U, with $(1/n)$ values less than 36, had 0.22% ²³⁵U content. Even the strongest ²³⁵U levels are not detected in these samples. Our thinnest samples of ²³²Th and ²³⁸U were obtained from the Oak Ridge National Laboratory isotopes division, and had less than 1 part in 6000 (isotopic) impurities. A thin Al coating was electrochemically deposited on these samples to prevent oxidation and corrosion. The natural radioactivity of our Th and U samples is not a factor in our transmission measurements. In our self-indication and capture measurements the net effect was small and could be treated as an additional contribution to natural background, even for ²³²Th, which tends to be a rather potent source of γ rays (unless a very recent chemical purification has been made to remove daughter activities).

The first step in the data processing involves determining the sample and energy-dependent

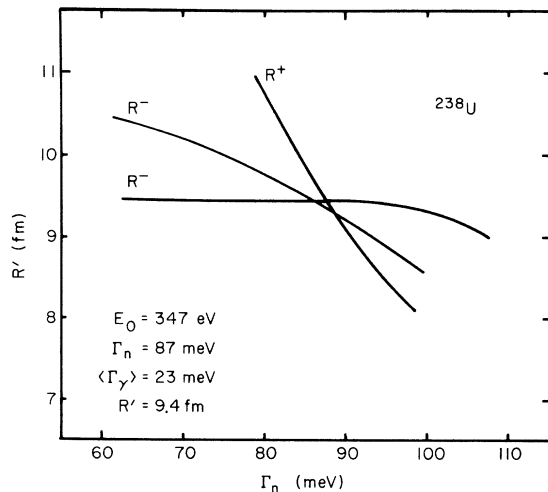


FIG. 5. Example of a plot of Γ_n versus R' for the 347-eV level in ²³⁸U. This technique is also used in the resonance-parameter analysis in favorable cases. R' is a local potential scattering radius, which includes contributions from other nearby resonances. The curves labeled R^+ is derived from the symmetric part of σ_t , using the Breit-Wigner single-level formalism. The curve labeled R^- comes from the antisymmetric part of σ_t , at points equidistant from the resonance energy E_0 . Values of σ_t are chosen where the cross section is not rapidly varying, such that resolution effects are relatively unimportant. The two R^+ curves are for different ΔE from exact resonance.

background rates as described in our erbium paper (VIII). The information is then put in a format of measured T and σ versus energy for each sample thickness. The measured σ values at resonance are distorted by resolution and sample-thickness-dependent effects. The subsequent analysis uses area and shape fit methods to find Γ_n and Γ_γ values most consistent with the data for each of the many sample thicknesses used. A sample of the T versus E values for two ²³²Th sample thicknesses for $500 \leq E \leq 700$ eV is given in the lower part of Fig. 2. The upper part of Fig. 2 shows an example of the self-indication data. The top histogram is the background-subtracted experimental count information for a “D-only” sample in the beam. The “D + T” histogram, which results from adding a thin transmission sample in the beam, is also shown. The addition of the T sample gives additional information in the low-energy region concerning the resonance parameters.

Examples of our background-subtracted M-R capture data for ²³²Th and ²³⁸U are shown in Fig. 3. This figure is for our thinnest samples in the region 400 to 1000 eV. To analyze the capture and “D-only” data, we determine the product of the absolute detector efficiency and the number of neutrons in the beam as a function of energy. The technique involved determining “absolute saturation” counting rates versus E for each sample as described in our previous papers.¹ This enables us to relate the experimentally observed total number of counts in a resonance, corrected for multiple interaction effects, to the resonance param-

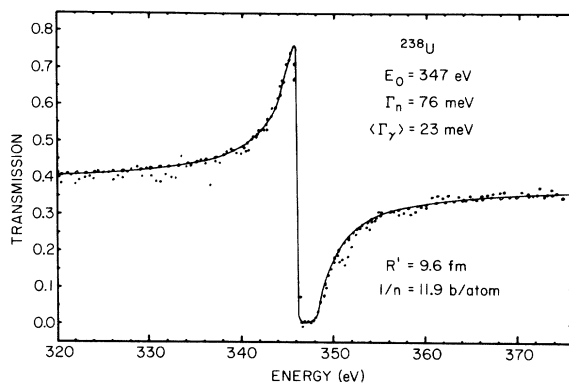


FIG. 6. Result of a shape analysis for the 347-eV level in ²³⁸U. The curve fits the data for the thick transmission sample with $1/n = 11.9$ b/atom. The analysis set Γ_γ equal to $\langle \Gamma_\gamma \rangle$ for ²³⁸U and a best fit was obtained by varying the parameters Γ_n and R' . For this level, contributions to R' from other levels are relatively small. Note that the parameters obtained are slightly different from those in Fig. 5, and that a still different “final choice” appears in Table III.

TABLE I. Neutron resonance parameters for assigned $l=0$ levels in ^{232}Th .

E_0 (eV)	ΔE_0	Γ_n^0 (meV)	$\Delta\Gamma_n^0$	Γ_γ	$\Delta\Gamma_\gamma$	E_0 (eV)	ΔE_0	Γ_n^0 (meV)	$\Delta\Gamma_n^0$	Γ_γ	$\Delta\Gamma_\gamma$
21.78	0.02	0.41	0.02	20.	2.	1039.13	0.37	0.45	0.05		
23.43	0.02	0.67	0.05	25.	2.	1064.54	0.38	0.13	0.02		
59.48	0.08	0.51	0.03	25.	2.	1077.20	0.39	0.37	0.06		
69.17	0.10	5.29	0.24	25.	2.	1093.26	0.39	0.05	0.01		
112.93	0.11	1.27	0.09	20.	2.	1109.6	0.4	0.69	0.05	17.	3.
120.78	0.11	2.18	0.14	22.	2.	1114.9	0.4	0.05	0.01		
129.10	0.13	0.30	0.02	18.	2.	1120.2	0.4	0.08	0.03		
154.24	0.16	0.01	0.002			1138.7	0.4	0.46	0.03	19.	3.
170.34	0.19	4.98	0.38	26.	2.	1150.2	0.4	0.59	0.05	22.	2.
192.57	0.23	1.33	0.07	17.	2.	1194.4	0.4	0.24	0.03		
196.13	0.24	0.005	0.001			1204.1	0.4	0.02	0.01		
199.30	0.24	0.89	0.07	18.	2.	1227.8	0.4	0.84	0.05	23.	3.
221.16	0.29	2.08	0.13	22.	2.	1243.1	0.4	0.54	0.06	20.	3.
251.48	0.18	2.02	0.13	24.	2.	1248.6	0.4	3.31	0.45	15.	3.
262.96	0.19	1.48	0.09	19.	2.	1269.4	0.5	0.55	0.04	20.	3.
285.74	0.21	1.77	0.10	20.	2.	1291.90	0.25	2.89	0.39	25.	2.
305.43	0.24	1.49	0.11	20.	2.	1301.61	0.26	1.44	0.14	21.	2.
328.92	0.26	4.19	0.33	26.	2.	1335.71	0.10	0.02	0.01		
341.83	0.28	1.95	0.11	19.	2.	1354.89	0.27	2.58	0.30	26.	2.
365.11	0.31	1.47	0.08	21.	2.	1359.82	0.28	0.28	0.02		
369.43	0.31	1.30	0.08	22.	2.	1372.54	0.28	0.02	0.01		
391.53	0.34	0.006	0.002			1377.85	0.28	1.43	0.19	24.	2.
400.86	0.36	0.52	0.05	18.	2.	1387.70	0.29	0.05	0.01		
411.62	0.36	0.007	0.002			1397.95	0.29	3.61	0.29	19.	2.
420.92	0.38	0.02	0.005			1426.43	0.30	2.70	0.24	21.	3.
454.1	0.4	0.05	0.01			1433.84	0.30	0.92	0.11	18.	3.
462.3	0.4	3.02	0.23	22.	2.	1461.28	0.31	0.03	0.01		
476.3	0.4	0.01	0.005			1478.15	0.31	0.05	0.01		
488.6	0.4	2.71	0.18	18.	2.	1508.60	0.32	0.02	0.01		
510.31	0.25	0.17	0.04			1518.60	0.33	4.62	0.64	24.	3.
528.46	0.26	0.52	0.04	20.	3.	1524.45	0.33	4.99	0.51	20.	3.
540.09	0.28	0.04	0.004			1555.56	0.34	0.17	0.02		
569.87	0.30	1.21	0.08	19.	2.	1581.41	0.35	0.53	0.04	20.	4.
573.46	0.30	0.03	0.01			1589.53	0.35	7.27	1.00	24.	2.
578.00	0.30	0.08	0.02			1602.63	0.35	1.22	0.15	24.	2.
598.16	0.32	0.39	0.04	19.	2.	1630.94	0.36	12.63	1.24	19.	5.
617.84	0.33	0.18	0.02			1640.35	0.37	1.09	0.12	25.	2.
656.41	0.36	1.99	0.16	20.	2.	1661.48	0.37	2.80	0.29	25.	4.
665.15	0.38	0.97	0.06	18.	2.	1677.73	0.38	0.61	0.07		
675.22	0.39	7.89	0.58	19.	2.	1696.90	0.38	0.04	0.01		
687.3	0.4	1.72	0.15	23.	2.	1704.97	0.38	0.06	0.01		
700.9	0.4	0.64	0.08	17.	4.	1719.72	0.39	0.82	0.07	17.	3.
712.8	0.4	0.82	0.11	19.	3.	1740.2	0.4	0.14	0.02		
740.9	0.4	6.98	0.55	23.	2.	1746.5	0.4	0.72	0.07	23.	4.
764.7	0.4	0.03	0.01			1762.6	0.4	2.43	0.40	27.	4.
778.5	0.4	0.39	0.03	26.	3.	1785.4	0.4	0.05	0.02		
804.1	0.5	6.35	0.46	20.	2.	1803.3	0.4	2.00	0.16	21.	3.
820.9	0.5	0.03	0.01			1811.9	0.4	1.06	0.14	20.	3.
836.6	0.5	0.04	0.01			1824.0	0.4	1.94	0.16	18.	3.
842.2	0.5	0.96	0.10	19.	2.	1848.6	0.4	0.13	0.02		
850.5	0.5	0.03	0.01			1854.4	0.4	1.04	0.16	25.	3.
866.2	0.5	0.44	0.07	23.	3.	1861.9	0.4	0.95	0.14	22.	3.
889.91	0.29	1.27	0.10	21.	2.	1899.9	0.4	2.87	0.32	29.	5.
905.97	0.30	0.05	0.01			1928.3	0.4	0.15	0.02		
926.47	0.31	0.007	0.003			1931.1	0.4	0.22	0.03		
943.22	0.31	1.47	0.16	23.	2.	1950.3	0.4	2.88	0.38	30.	4.
962.55	0.33	0.17	0.02			1971.2	0.4	5.52	0.52	25.	4.
982.65	0.33	1.02	0.10	21.	2.	1987.8	0.4	0.96	0.11	18.	3.
990.46	0.34	2.22	0.16	25.	4.	2004.9	0.4	0.51	0.07	22.	4.
1010.39	0.35	3.55	0.47	20.	3.	2051.7	0.5	0.42	0.07		

TABLE I (Continued)

E_0 (eV)	ΔE_0	Γ_n^0 (meV)	$\Delta\Gamma_n^0$	Γ_γ (meV)	$\Delta\Gamma_\gamma$	E_0 (eV)	ΔE_0	Γ_n^0 (meV)	$\Delta\Gamma_n^0$	Γ_γ (meV)	$\Delta\Gamma_\gamma$
2061.9	0.5	1.43	0.18	17.	3.	3027.3	0.9	4.18	0.45		
2073.8	0.5	0.15	0.04			3039.7	0.9	1.07	0.09		
2079.0	0.5	0.20	0.04			3050.2	0.9	0.09	0.05		
2097.3	0.5	0.02	0.01			3061.4	0.9	0.52	0.05		
2116.9	0.5	1.63	0.13	20.	3.	3082.8	0.9	0.99	0.11		
2147.6	0.5	1.92	0.15	14.	4.	3103.6	0.9	0.03	0.01		
2162.9	0.5	1.87	0.15	26.	4.	3109.2	0.9	0.39	0.05		
2177.9	0.5	1.59	0.13	17.	3.	3120.7	0.9	0.13	0.04		
2196.9	0.5	1.00	0.11	17.	3.	3148.5	0.9	3.30	0.36		
2216.2	0.5	0.49	0.04			3153.4	0.9	3.47	0.36		
2222.0	0.5	1.80	0.19	27.	5.	3163.0	0.9	0.37	0.07		
2233.5	0.5	0.03	0.01			3188.6	0.9	1.33	0.12		
2270.9	0.5	0.59	0.08			3194.5	0.9	0.07	0.05		
2276.3	0.6	0.96	0.10	24.	3.	3207.4	0.9	1.59	0.18		
2286.4	0.6	5.44	0.63	19.	5.	3229.4	1.0	0.30	0.05		
2320.9	0.6	0.09	0.03			3242.5	1.0	0.25	0.05		
2336.0	0.6	2.28	0.37	20.	4.	3252.7	1.0	1.46	0.14		
2344.4	0.6	0.09	0.04			3270.0	1.0	0.45	0.07		
2352.5	0.6	0.31	0.06			3295.7	1.0	7.11	0.78		
2353.7	0.6	0.29	0.06			3307.2	1.0	0.07	0.07		
2375.2	0.6	2.42	0.37	18.	3.	3317.6	1.0	0.09	0.05		
2382.8	0.6	0.04	0.02			3331.8	1.0	0.71	0.10		
2391.1	0.6	0.07	0.02			3342.9	1.0	2.94	0.31		
2418.5	0.6	1.75	0.18			3351.4	1.0	0.31	0.07		
2439.8	0.6	0.21	0.03			3383.5	1.0	1.20	0.15		
2455.8	0.6	3.53	0.44			3409.5	1.0	0.08	0.03		
2474.9	0.6	0.04	0.02			3442.9	1.1	0.34	0.05		
2491.8	0.6	0.13	0.03			3471.9	1.1	0.31	0.05		
2509.3	0.6	6.29	0.70			3510.0	1.1	0.08	0.05		
2527.3	0.6	0.93	0.12			3521.8	1.1	1.79	0.30		
2557.1	0.7	0.07	0.02			3544.2	1.1	0.12	0.05		
2563.1	0.7	6.12	0.59			3574.4	1.1	0.28	0.05		
2569.6	0.7	1.18	0.20			3594.4	1.1	0.35	0.07		
2612.5	0.7	1.70	0.20			3611.6	1.1	2.00	0.25		
2624.3	0.7	0.14	0.04			3623.5	1.1	0.20	0.05		
2635.0	0.7	3.12	0.35			3636.7	1.2	0.13	0.05		
2655.5	0.7	0.09	0.04			3651.7	1.2	1.11	0.13		
2663.4	0.7	3.88	0.39			3674.2	1.2	0.20	0.05		
2677.0	0.7	0.23	0.04			3692.7	1.2	0.10	0.07		
2688.4	0.7	3.80	0.39			3707.6	1.2	0.08	0.05		
2713.0	0.7	1.84	0.23			3716.0	1.2	0.43	0.07		
2722.7	0.7	0.22	0.04			3722.9	1.2	1.61	0.33		
2733.2	0.7	6.89	0.57			3732.8	1.2	0.79	0.11		
2748.1	0.7	0.29	0.06			3745.2	1.2	0.08	0.05		
2773.6	0.8	1.52	0.25			3759.2	1.2	0.13	0.05		
2792.9	0.8	3.12	0.36			3786.4	1.2	0.47	0.08		
2815.6	0.8	0.55	0.08			3799.4	1.2	0.08	0.05		
2832.9	0.8	0.70	0.09			3820.5	1.2	0.65	0.10		
2838.7	0.8	0.03	0.03			3827.0	1.3	1.76	0.27		
2852.0	0.8	3.93	0.56			3848.5	1.3	0.19	0.06		
2883.9	0.8	0.08	0.03			3868.8	1.3	1.05	0.13		
2895.9	0.8	0.04	0.01			3883.4	1.3	0.18	0.05		
2915.6	0.8	0.06	0.02			3906.0	1.3	3.52	0.48		
2948.6	0.8	1.77	0.18			3923.4	1.3	0.14	0.05		
2956.5	0.8	0.81	0.11			3931.5	1.3	0.59	0.10		
2966.2	0.8	0.26	0.06			3951.1	1.3	0.16	0.06		
2980.0	0.8	0.16	0.04			3961.4	1.3	0.65	0.10		
2988.0	0.9	0.68	0.11			3970.3	1.3	1.14	0.14		
3006.5	0.9	0.03	0.01			3976.5	1.3	1.90	0.27		
3017.3	0.9	0.51	0.05			3994.4	1.3	0.57	0.09		

ters. The ratios of the “ $D+T$ ” to the “ D -only” data gives other relationships. Thus, for each resonance, each independent analysis yields a different implied relationship between Γ_n and Γ_γ as shown in Fig. 4 for one level each in ^{232}Th and ^{238}U . Multiple-scattering corrections for both the M-R and the self-indication data have been included in these curves. The common intersection of the curves gives the resonance parameters (Γ_n, Γ_γ) and an indication of the uncertainty in these parameters. In addition to the area analysis, we use a partial shape analysis of the thickest sample ($1/n = 11.9$) transmission data in determining the resonance parameters. Figure 5 is an example of this analysis for the 347-eV level in ^{238}U . We have plotted Γ_n versus R' in this figure, where R' is a (local) potential scattering radius, which includes effects of other nearby resonances, may be slightly energy-dependent within a resonance, and varies from resonance to resonance. The curve which is relatively independent of Γ_n is from the wings where mainly potential scattering applies. The R^+ and R^- are derived from the symmetric and anti-symmetric parts of σ_i at distances on either side of exact resonance corresponding to the interference minima on the low-energy side of resonance. The common intersection of curves determines R' and Γ_n if $\Gamma_n \gg \Gamma_\gamma$.

In places where contributions from nearby resonances are negligible, R' derived from this analysis is the effective potential scattering radius derived from the optical model. Interference contributions from more than one resonance are significant except in the vicinity of a few single isolated resonances, notably 221 eV in ^{232}Th and 347 eV in ^{238}U . At these energy regions one can ex-

amine the behavior of the cross section, particularly at the interference minimum and in the wings where σ is sensitive to R' , and resolution effects are relatively unimportant. Figure 6 shows a fit of σ versus E in the vicinity of the 347-eV level in ^{238}U . From these figures we arrive at $R' = 9.6 \pm 0.3$ fm for ^{238}U . The uncertainty is due to a systematic uncertainty in the transmission estimated at $\pm 3\%$, which corresponds to ± 0.3 fm in R' . Our value compares with a value of $R' = 9.11$ fm obtained by Divadeenam.¹⁷ For ^{232}Th we find that $R' = 9.1 \pm 0.3$ fm from a similar analysis. This compares with Ribon's¹⁰ value of $R' = (9.65 \pm 0.10)$ fm and $R' = 9.04$ fm reported by Divadeenam.¹⁷ Additional details on the analysis can be found in our previous papers.

IV. RESULTS

The results of our data analysis for the resonance parameters for ^{232}Th are given in Tables I and II, where Table I is for levels considered to be s wave, and Table II is for levels considered to be p wave. The similar s - and p -level results for ^{238}U are given in Tables III and IV. The basis for the selection of the s population is given in Ref. 9, along with the actual selections, although the final Γ_n and Γ_γ values had not been established at that time. The calculation of the p reduced neutron width, $g\Gamma_n^1 \equiv g\Gamma_n(E_1/E)^{1/2}$, depends on the choice of an effective nuclear radius R . E_1 is the “barrier energy” where χ of the neutron equals R . We use $R = 1.41A^{1/3}$ fm (8.67 fm for ^{232}Th and 8.74 fm for ^{238}U), giving $E_1 = 276$ keV and 270 keV for ^{232}Th and ^{238}U , respectively. The statistical spin factor g is included, and is unity except for $p_{3/2}$ levels where it is equal to 2. Table V summarizes our average values for the s -level

TABLE II. Neutron resonance parameters for $l=1$ levels in ^{232}Th . $g=1$ and 2 for $p_{1/2}$ and $p_{3/2}$, respectively.

E_0 (eV)	ΔE_0	$g\Gamma_n^1$ (meV)	$\Delta g\Gamma_n^1$	E_0 (eV)	ΔE_0	$g\Gamma_n^1$ (meV)	$\Delta g\Gamma_n^1$	E_0 (eV)	ΔE_0	$g\Gamma_n^1$ (meV)	$\Delta g\Gamma_n^1$	E_0 (eV)	ΔE_0	$g\Gamma_n^1$ (meV)	$\Delta g\Gamma_n^1$
58.84	0.07	3.6	1.8	380.40	0.33	4.0	1.3	1217.3	0.4	3.9	1.4	1897.1	0.4	6.5	2.6
90.08	0.08	3.2	1.6	402.62	0.36	3.0	1.5	1223.8	0.4	2.6	1.2	2015.4	0.4	2.4	1.3
128.21	0.12	8.5	2.0	533.55	0.27	4.9	1.7	1233.3	0.4	4.8	1.7	2055.5	0.5	1.5	0.8
145.72	0.15	14.1	3.0	535.45	0.27	7.1	2.0	1260.8	0.5	3.7	1.3	2158.5	0.5	5.5	2.3
178.62	0.21	6.9	2.2	660.66	0.37	3.2	1.3	1261.7	0.5	5.6	1.8	2170.1	0.5	7.9	2.9
202.41	0.25	2.8	1.4	771.7	0.4	1.9	1.0	1287.84	0.25	3.0	1.3	2206.8	0.5	5.6	2.4
210.87	0.26	1.8	0.9	846.7	0.5	1.6	0.8	1345.65	0.27	5.3	2.0	2307.2	0.5	7.6	2.9
219.30	0.28	1.7	0.9	869.3	0.5	7.7	2.8	1349.44	0.27	4.4	1.6	2329.5	0.6	4.9	2.1
242.23	0.16	2.1	1.1	919.26	0.30	2.9	1.4	1384.59	0.29	1.6	0.9	2427.4	0.6	5.5	2.4
290.12	0.21	2.2	1.1	934.24	0.31	1.9	0.9	1441.30	0.30	6.1	2.5	2434.6	0.6	6.8	3.0
302.30	0.23	5.2	2.2	1021.38	0.35	2.9	1.3	1469.27	0.31	1.4	0.8	2462.5	0.6	8.0	3.2
309.20	0.24	3.0	1.4	1043.74	0.37	5.3	2.0	1509.56	0.32	16.6	3.4	2604.0	0.7	3.3	1.7
321.47	0.25	1.9	1.0	1073.73	0.39	1.6	0.8	1610.47	0.36	3.5	1.5	2803.4	0.8	8.5	3.5
338.26	0.26	2.6	1.3	1115.9	0.4	8.0	2.4	1689.65	0.38	5.9	2.1	2843.2	0.8	2.7	1.4
361.47	0.31	3.2	1.6	1132.7	0.4	2.2	1.1	1767.1	0.4	5.5	2.2	2861.2	0.8	14.5	5.0
												2870.4	0.8	2.7	1.5
												2932.0	0.8	2.7	1.5

TABLE III. Neutron resonance parameters for assigned $l=0$ levels in ^{238}U .

E_0 (eV)	ΔE_0	Γ_n^0 (meV)	$\Delta\Gamma_n^0$	Γ_γ	$\Delta\Gamma_\gamma$ (meV)	E_0 (eV)	ΔE_0	Γ_n^0 (meV)	$\Delta\Gamma_n^0$	Γ_γ	$\Delta\Gamma_\gamma$ (meV)
6.65	0.10	0.59	0.02			1244.9	0.5	7.94	0.99	24.	2.
20.90	0.10	1.86	0.17	22.	3.	1266.8	0.6	0.62	0.08	21.	2.
36.80	0.07	6.26	0.33	23.	2.	1272.7	0.6	0.76	0.08	24.	2.
66.10	0.15	3.20	0.25	21.	2.	1298.1	0.3	0.12	0.03		
80.70	0.07	0.19	0.02			1316.5	0.3	0.11	0.02		
102.47	0.09	6.92	0.40	28.	3.	1332.7	0.6	0.04	0.02		
116.82	0.11	3.24	0.28	20.	2.	1363.4	0.6	0.03	0.01		
145.57	0.15	0.07	0.004			1393.2	0.3	4.88	0.54	28.	3.
165.21	0.19	0.24	0.03	18.	5.	1405.2	0.3	1.87	0.21	25.	2.
189.80	0.23	12.99	1.09	27.	3.	1419.2	0.3	0.24	0.03		
208.49	0.25	4.09	0.42	22.	4.	1427.4	0.4	0.77	0.08	26.	3.
237.20	0.16	2.27	0.26	24.	3.	1443.5	0.4	0.47	0.08	22.	3.
263.91	0.19	0.01	0.002			1473.4	0.4	3.26	0.26	28.	3.
273.56	0.20	1.75	0.18	23.	3.	1522.3	0.4	6.15	0.38	30.	7.
291.01	0.21	1.00	0.12	22.	3.	1532.3	0.4	0.01	0.01		
311.13	0.25	0.06	0.01			1545.8	0.4	0.06	0.03		
347.74	0.28	4.30	0.35	26.	3.	1565.1	0.4	0.11	0.04		
377.03	0.32	0.05	0.01			1597.5	0.5	8.88	0.63	20.	4.
397.39	0.35	0.30	0.03	22.	6.	1622.3	0.5	1.74	0.35	19.	3.
410.18	0.36	0.94	0.10	18.	2.	1637.4	0.5	1.24	0.20	19.	3.
433.7	0.4	0.42	0.05	20.	2.	1662.0	0.5	4.17	0.49	24.	4.
454.1	0.4	0.02	0.005			1688.3	0.5	2.24	0.24	19.	3.
462.8	0.4	0.21	0.02			1709.0	0.5	2.03	0.19	28.	5.
477.0	0.4	0.14	0.02			1722.2	0.5	0.36	0.05		
518.27	0.25	2.15	0.22	24.	2.	1755.2	0.5	2.51	0.24	27.	4.
535.21	0.25	1.95	0.22	23.	2.	1782.1	0.5	15.87	1.90		
555.90	0.30	0.03	0.01			1795.5	0.5	0.07	0.02		
579.87	0.30	1.70	0.17	21.	2.	1807.9	0.5	0.34	0.08	17.	5.
594.84	0.31	3.49	0.21	20.	2.	1845.5	0.5	0.30	0.12	15.	5.
619.75	0.35	1.12	0.12	19.	2.	1868.0	0.5	0.09	0.05		
628.29	0.35	0.21	0.02			1870.0	0.5	0.07	0.04		
660.9	0.4	5.37	0.58	29.	3.	1902.4	0.5	0.78	0.09	19.	4.
692.9	0.4	1.60	0.19	22.	2.	1916.5	0.5	0.57	0.07	19.	5.
707.9	0.4	0.79	0.08	21.	2.	1953.4	0.5	0.07	0.02		
720.9	0.4	0.05	0.01			1968.6	0.5	14.99	2.70	30.	10.
732.5	0.4	0.04	0.01			1974.3	0.5	11.59	1.80		
764.8	0.5	0.29	0.04	17.	2.	2022.8	0.6	4.67	0.67	20.	4.
778.8	0.5	0.06	0.01			2029.8	0.6	1.35	0.40	18.	5.
790.4	0.5	0.21	0.01			2070.9	0.6	0.007	0.004		
820.9	0.5	2.27	0.17	20.	2.	2088.1	0.6	0.50	0.11	22.	4.
850.6	0.5	1.89	0.17	23.	2.	2095.9	0.6	0.28	0.07		
856.1	0.5	2.77	0.24	23.	2.	2123.8	0.6	0.07	0.03		
866.0	0.5	0.17	0.02			2144.6	0.6	1.34	0.17	15.	5.
904.5	0.3	1.63	0.10	22.	2.	2152.2	0.6	5.17	0.75	32.	8.
924.5	0.3	0.32	0.03	25.	4.	2186.0	0.6	13.26	1.71	29.	7.
936.6	0.3	4.71	0.39	25.	2.	2200.6	0.6	2.45	0.36	26.	5.
958.0	0.4	6.56	0.65	21.	2.	2229.3	0.6	0.68	0.02		
991.4	0.4	12.39	0.79	30.	5.	2235.1	0.6	0.10	0.02		
1010.5	0.4	0.05	0.02			2258.8	0.6	1.81	0.32		
1022.9	0.4	0.26	0.05			2265.9	0.7	4.41	0.63	20.	5.
1028.6	0.5	0.08	0.03			2281.7	0.7	2.83	0.42	18.	5.
1054.0	0.5	2.74	0.25	27.	2.	2314.5	0.7	0.44	0.08		
1098.1	0.5	0.51	0.09	22.	3.	2336.9	0.7	0.17	0.08		
1108.9	0.5	0.81	0.12	24.	2.	2352.8	0.7	0.97	0.21	28.	5.
1131.1	0.5	0.05	0.02			2355.3	0.7	1.26	0.21	24.	5.
1139.9	0.5	6.52	0.59	23.	2.	2391.4	0.7	0.53	0.08		
1166.9	0.5	2.49	0.15	23.	2.	2410.8	0.7	0.08	0.04		
1176.6	0.5	1.75	0.15	22.	2.	2425.7	0.7	2.84	0.37		
1194.5	0.5	2.58	0.14	19.	2.	2445.5	0.7	3.94	0.51		
1210.5	0.5	0.20	0.02			2454.8	0.7	0.38	0.06		

TABLE III (Continued)

E_0 (eV)	ΔE_0	Γ_n^0 (meV)	$\Delta\Gamma_n^0$	Γ_γ $\Delta\Gamma_\gamma$ (meV)	E_0 (eV)	ΔE_0	Γ_n^0 (meV)	$\Delta\Gamma_n^0$	Γ_γ $\Delta\Gamma_\gamma$ (meV)
2488.4	0.7	1.66	0.18		3355.1	1.2	1.86	0.26	
2520.7	0.8	0.16	0.06		3388.3	1.2	0.25	0.07	
2547.2	0.8	10.90	0.99		3407.9	1.2	3.25	0.51	
2558.5	0.8	4.55	0.59		3417.7	1.2	0.07	0.05	
2579.9	0.8	6.69	0.59		3435.3	1.2	5.97	0.68	
2596.5	0.8	14.52	0.88		3456.3	1.3	9.53	0.85	
2619.1	0.8	0.88	0.16		3484.3	1.3	1.78	0.42	
2631.7	0.8	0.04	0.02		3493.3	1.3	0.16	0.07	
2671.3	0.9	5.22	0.39		3526.4	1.3	0.07	0.05	
2695.6	0.9	0.37	0.08		3560.5	1.3	3.69	0.50	
2716.5	0.9	2.78	0.38		3572.7	1.3	5.52	0.50	
2728.4	0.9	0.04	0.04		3593.3	1.3	0.83	0.10	
2749.7	0.9	0.86	0.15		3621.8	1.3	0.15	0.07	
2761.6	0.9	0.44	0.10		3628.3	1.4	6.97	0.66	
2786.0	0.9	0.23	0.06		3671.8	1.4	0.13	0.08	
2805.4	0.9	0.08	0.04		3692.0	1.4	5.27	0.66	
2828.4	0.9	0.33	0.07		3715.5	1.4	1.23	0.41	
2864.1	0.9	3.27	0.56		3733.0	1.4	3.19	0.65	
2881.8	0.9	10.25	0.75		3763.6	1.5	1.17	0.20	
2896.3	0.9	0.22	0.11		3780.8	1.5	5.77	0.98	
2933.9	1.0	0.57	0.07		3830.3	1.5	0.11	0.06	
2955.7	1.0	0.39	0.09		3856.4	1.5	7.97	0.81	
2965.8	1.0	0.06	0.03		3872.1	1.5	2.73	0.80	
2986.3	1.0	0.10	0.04		3901.3	1.5	4.32	0.96	
3002.4	1.0	2.14	0.27		3913.4	1.5	1.44	0.24	
3015.1	1.0	0.03	0.02		3939.0	1.5	2.07	0.32	
3027.8	1.0	2.27	0.36		3953.9	1.5	1.72	0.24	
3042.5	1.0	0.04	0.02		4040.4	1.5	1.02	0.16	
3058.1	1.0	0.58	0.14		4063.0	1.5	0.47	0.13	
3108.8	1.0	3.59	0.54		4089.4	1.6	1.13	0.23	
3132.6	1.0	0.11	0.05		4124.0	1.6	0.50	0.12	
3148.1	1.1	1.51	0.25		4167.8	1.6	2.48	0.54	
3168.5	1.1	0.14	0.05		4178.2	1.7	0.59	0.14	
3177.8	1.1	1.31	0.23		4209.4	1.7	0.62	0.14	
3188.1	1.1	1.42	0.25		4257.7	1.7	0.26	0.11	
3204.9	1.1	1.29	0.23		4299.0	1.7	2.01	0.27	
3217.0	1.1	0.14	0.07		4306.0	1.7	1.75	0.26	
3224.9	1.1	0.58	0.14		4323.9	1.7	0.94	0.15	
3248.1	1.1	0.49	0.11		4333.2	1.8	0.05	0.03	
3272.0	1.1	0.07	0.03		4396.4	1.8	2.12	0.23	
3278.2	1.1	4.19	0.52		4435.0	1.8	1.58	0.38	
3295.2	1.1	0.08	0.03		4487.2	1.8	0.04	0.03	
3310.3	1.1	2.14	0.35		4510.3	1.8	7.52	1.19	
3320.2	1.2	1.79	0.35		4542.0	1.8	1.11	0.18	
3332.9	1.2	1.21	0.17		4567.2	1.8	0.50	0.12	
					4592.7	1.9	0.27	0.09	

strength function, S_0 , $\langle\Gamma_n^0\rangle$, and the average capture width, $\langle\Gamma_\gamma\rangle$, for the levels for which Γ_γ is determined.

Figure 7 shows the cumulative number of levels N versus E , and the plots for only s levels versus E as obtained in Ref. 9. For s levels only, $\langle D \rangle = (16.7 \pm 0.2)$ eV for ^{232}Th and (20.8 ± 0.3) eV for ^{238}U , where a fractional uncertainty $2/n$ is given in each case (n = number of levels).

The plots of $\sum\Gamma_n^0$ versus E for ^{232}Th and ^{238}U are shown in Fig. 8. The slopes of these plots are in-

sensitive to inclusion of weak p levels and give the s strength function. Most emphasis is given to the regions below about 3.5 keV in ^{232}Th and 4.0 keV in ^{238}U . Our level analysis was actually made to higher energies than shown in the tables and figures, with a considerably smaller slope for $\sum\Gamma_n^0$ above these energies. Since the analysis above these energies was less reliable, and perhaps misleading, we omit the higher energy values. In this connection, it now seems that similar analysis difficulties occurred in our earlier ^{232}Th

TABLE IV. Neutron resonance parameters for $l=1$ levels in ^{238}U . $g=1$ and 2 for $p_{1/2}$ and $p_{3/2}$, respectively.

E_0 (eV)	ΔE_0	$g\Gamma_n^1$ (meV)	$\Delta g\Gamma_n^1$	E_0 (eV)	ΔE_0	$g\Gamma_n^1$ (meV)	$\Delta g\Gamma_n^1$	E_0 (eV)	ΔE_0	$g\Gamma_n^1$ (meV)	$\Delta g\Gamma_n^1$	E_0 (eV)	ΔE_0	$g\Gamma_n^1$ (meV)	$\Delta g\Gamma_n^1$
10.22	0.01	14.6	3.0	337.19	0.27	2.2	1.1	846.9	0.4	11.0	3.3	1256.5	0.4	1.2	0.9
19.50	0.02	4.3	1.8	351.75	0.30	3.3	1.5	890.6	0.3	8.0	2.7	1371.6	0.3	3.2	1.7
45.19	0.07	1.8	0.9	354.66	0.31	1.2	0.8	909.5	0.3	12.7	3.5	1381.6	0.3	3.1	1.6
63.54	0.08	3.2	1.4	407.64	0.36	2.7	1.4	932.3	0.3	2.9	1.6	1410.5	0.3	2.0	1.2
83.57	0.08	1.4	0.7	439.71	0.39	4.7	2.1	940.1	0.3	2.9	1.5	1416.3	0.3	8.9	2.7
89.19	0.08	28.8	3.5	488.20	0.40	11.2	3.4	964.9	0.3	1.8	1.1	1549.8	0.3	5.3	2.3
121.61	0.11	1.2	0.7	498.93	0.25	2.0	1.1	976.8	0.3	5.3	1.9	1646.1	0.3	3.9	2.1
124.30	0.12	2.3	1.2	523.21	0.26	4.5	2.0	985.6	0.3	2.6	1.4	1744.9	0.4	7.3	2.6
152.42	0.16	5.7	2.2	542.34	0.28	1.1	0.8	1014.4	0.3	13.2	3.0	1912.6	0.4	1.6	1.0
158.89	0.17	0.9	0.7	606.12	0.33	4.5	2.2	1031.1	0.3	8.1	2.7	2175.2	0.5	3.9	2.0
173.11	0.19	3.0	1.3	624.80	0.34	17.3	3.8	1062.3	0.3	5.4	2.5	2288.9	0.6	2.2	1.2
202.30	0.25	3.7	1.5	668.40	0.37	3.9	1.8	1067.6	0.3	7.7	2.1	2798.1	0.8	3.7	1.9
214.97	0.27	3.4	1.4	677.50	0.39	10.6	3.1	1071.0	0.3	2.4	1.3	2907.1	0.8	2.6	1.5
242.60	0.16	10.6	2.4	712.49	0.40	3.6	1.5	1081.0	0.3	5.3	2.5	2922.1	0.8	6.8	2.7
253.88	0.18	6.6	2.0	729.4	0.4	9.4	2.9	1094.4	0.4	9.6	2.9				
255.37	0.19	4.0	1.7	743.2	0.4	3.9	1.6	1102.7	0.4	14.6	3.5				
257.10	0.19	1.3	0.8	756.0	0.4	5.7	2.6	1147.0	0.4	2.1	1.1				
275.76	0.20	4.7	2.1	808.2	0.4	4.7	2.3	1154.8	0.4	2.8	1.4				
282.29	0.21	3.5	1.5	815.3	0.4	2.3	1.2	1217.9	0.4	2.5	1.4				
294.96	0.22	1.6	0.9	832.4	0.4	2.9	1.5	1237.9	0.4	2.5	1.3				

and ^{238}U studies with increasing tendency to underestimate Γ_n^0 values for $E > 1$ keV, with resulting too small values for S_0 . Our best judgement choices for the s strength function, with fractional uncertainties of $\pm 1.4/\sqrt{n}$, are:

$$10^4 S_0 = (0.84 \pm 0.08) \text{ for } ^{232}\text{Th} \text{ to } 3.5 \text{ keV};$$

$$10^4 S_0 = (1.08 \pm 0.10) \text{ for } ^{238}\text{U} \text{ to } 4.0 \text{ keV}.$$

The best previous work on the neutron widths and strength function of ^{232}Th was done at Saclay and Harwell. Ribon¹⁰ at Saclay obtained parameters up to 3 keV using a 103 m flight path and samples cooled to 77°K. He was able to detect considerably more of the weaker p levels than we observed. For the s strength function, Ribon obtained $10^4 S_0 = (0.87 \pm 0.10)$. Asghar *et al.*¹¹ at Harwell published their ^{232}Th results in 1966 for data obtained from 15 eV to 1 keV, using the 120- and

192-m flight path of their electron linac. They obtained $10^4 S_0 = (0.80 \pm 0.17)$ which is the same as our result for this interval. Both these values are consistent with our value for the range 0 to 4 keV of (0.84 ± 0.08) . The Harwell group of Asghar, Chaffey, and Moxon¹² also reported a value of $(0.70_{-0.10}^{+0.15})$ for the s strength function in ^{238}U (6- to 823-eV region). This is lower than our present choice for S_0 in the full energy interval to 4.6 keV, but Fig. 8(b) shows that $\sum \Gamma_n^0$ to 840 eV is very non-linear and has lower average slope than for the interval to 4.6 keV. Carraro and Kolar¹⁴ at the Geel Linac found $10^4 S_0 = (1.13 \pm 0.13)$ for essentially the same energy interval which we emphasize. They tend to obtain Γ_n^0 values systematically higher than our values. They also give values for $\langle D \rangle$ and $\langle \Gamma_n^0 \rangle$ for "s levels only" but their criterion for s versus p behavior is rather arbitrary and quite different from ours.

TABLE V. Average parameters for our selected s -wave levels.

Energy interval (keV)	^{232}Th				^{238}U			
	$\langle \Gamma_n^0 \rangle$ (meV)	$S_0 \times 10^{-4}$	$\langle \Gamma_n \rangle$ (meV)	ν	$\langle \Gamma_n^0 \rangle$ (meV)	$S_0 \times 10^{-4}$	$\langle \Gamma_n \rangle$ (meV)	ν
0-1	1.35 ± 0.24	0.80 ± 0.14	21.05	129	2.15 ± 0.43	1.03 ± 0.20	22.59	105
1-2	1.49 ± 0.26	0.88 ± 0.16	21.88	82	2.36 ± 0.46	1.13 ± 0.22	23.00	70
2-3	1.36 ± 0.24	0.82 ± 0.15	20.08	58	2.36 ± 0.46	1.13 ± 0.22	22.90	43
3-4	0.90 ± 0.16	0.56 ± 0.12			2.13 ± 0.42	1.02 ± 0.21		
4-4.6						0.41 ± 0.12		
Best choice value	1.40 ± 0.15	0.84 ± 0.08	21.2 ± 0.3		2.24 ± 0.23	1.08 ± 0.10	22.9 ± 0.5	

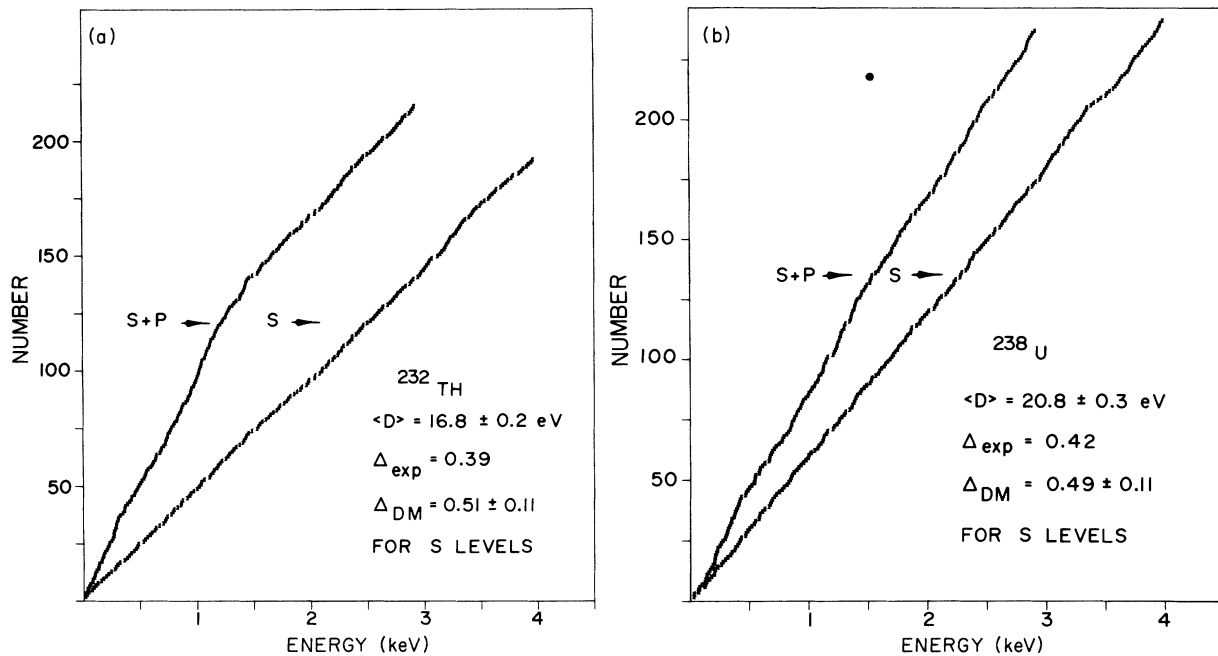


FIG. 7. (a), (b) Plots of N versus E for the resonances observed in ^{232}Th and ^{238}U . Good fits to a straight line are obtained for the s population up to 3 keV, and the agreement of our Δ_{exp} and the theoretical Δ_{DM} are shown.

The comparison of our new distributions of $y = (\Gamma_n^0)^{1/2}$ for the s -level populations of ^{232}Th and ^{238}U with theory are shown in Fig. 9. It is seen that the fits to the Porter-Thomas (P.T.) single-channel curves are reasonably close. The extra weak p levels all have $g\Gamma_n$ values that would place them in the lowest histogram box if treated as s levels. In Ref. 9, before final Γ_n^0 values were obtained for this data, but using the results for the positions and relative strengths of the levels to

supplement our older results for the main s population of stronger levels, we applied various tests to "select" the ^{232}Th and ^{238}U s population to 3 keV. One important factor of those choices was to keep, as s levels, numbers of weak levels in reasonable agreement with the P.T. single-channel-theory prediction. The selected s populations were then found to give good agreement with the tests for the statistical O.E. theory for the level-spacing systematics. The details are given in Ref. 9. The

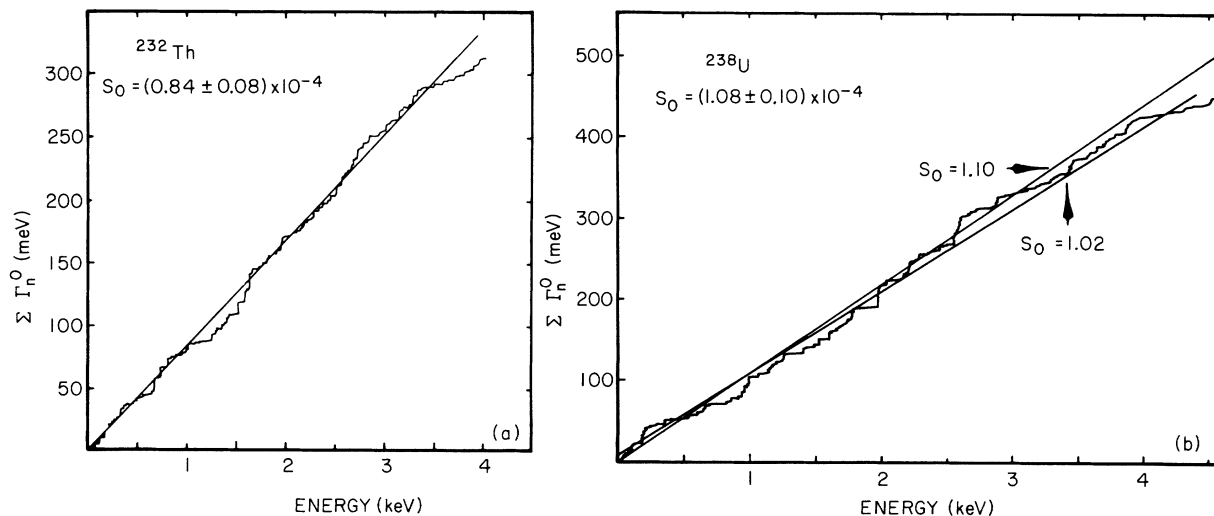


FIG. 8. (a), (b) Plots of $\sum \Gamma_n^0$ versus E for ^{232}Th and ^{238}U . The slopes of the curves determine the s -wave strength functions.

distributions of Fig. 9 use the s population choices of Ref. 9. Maximum likelihood analyses for the 178 s levels of ^{232}Th below 3 keV give $\nu = (1.11 \pm 0.11)$ degrees of freedom, while similar analyses for the 146 s levels of ^{238}U give $\nu = (1.04 \pm 0.11)$. Both values are quite consistent with $\nu = 1$.

Since there has been some discussion in the literature¹⁵ as to whether or not ^{232}Th satisfies the P.T. single-channel theory for the Γ_n^0 values, particularly below 500 eV, we show plots for ^{232}Th and ^{238}U of the cumulative value of ν versus E in Fig. 10. It is seen that ν has a peak of about 2.7 near 400 eV for ^{232}Th which is the effect discussed. We have no satisfactory explanation for this effect. The value of ν for ^{238}U remains closer to unity over the full region, but has a smaller rise above unity below 500 eV to which we attach no special significance.

It seems difficult to deny that the neutron channel at low energy is in fact a "single channel." The logical question is whether or not the true intrinsic S_0 fluctuates over the region (intermediate structure effects), or whether or not the observed deficiency of weak s levels in this interval represents a breakdown in the P.T. theory for what is clearly a single-channel process. Ribon presents a diagram of "observed $g\Gamma_n^0$ " for all observed levels in ^{232}Th versus energy, with a logarithmic

scale of $g\Gamma_n^0$ (the analysis is made as if all levels had $l=0$). He chose a higher band of $g\Gamma_n^0$ levels as s levels and a lower band of $g\Gamma_n^0$ as p levels or uncertain. He picked an upper limit for the $g\Gamma_n^0$ value of p levels for which there is 10^{-4} probability of obtaining a value below that limit. Below 500 eV there was a region below $g\Gamma_n^0 = 0.3$ meV, but above the p -wave upper-limit curve there were no observed levels, where ~ 6 levels would have been expected on average. He concludes that the probability for this situation is $\sim 10^{-3}$. A similar division method was used by Forman *et al.*¹⁵ to separate the s and p populations. In both cases, the separation of p levels from the stronger s levels should be good, but the peaking of the P.T. distribution near zero prevents them from correctly separating weak s levels from p levels.

An excess of weak levels was observed both for ^{232}Th and ^{238}U over the number of levels expected for the s population alone. These are considered to be p levels, with a possible inclusion of a few spurious "noise" fluctuations as levels. The information from the $g\Gamma_n^1$ values for these levels permits us to make a rough estimate of the p strength function S_1 , for the two isotopes. In making such estimates it must be noted that: (a) Most of the p levels are too weak for us to observe;

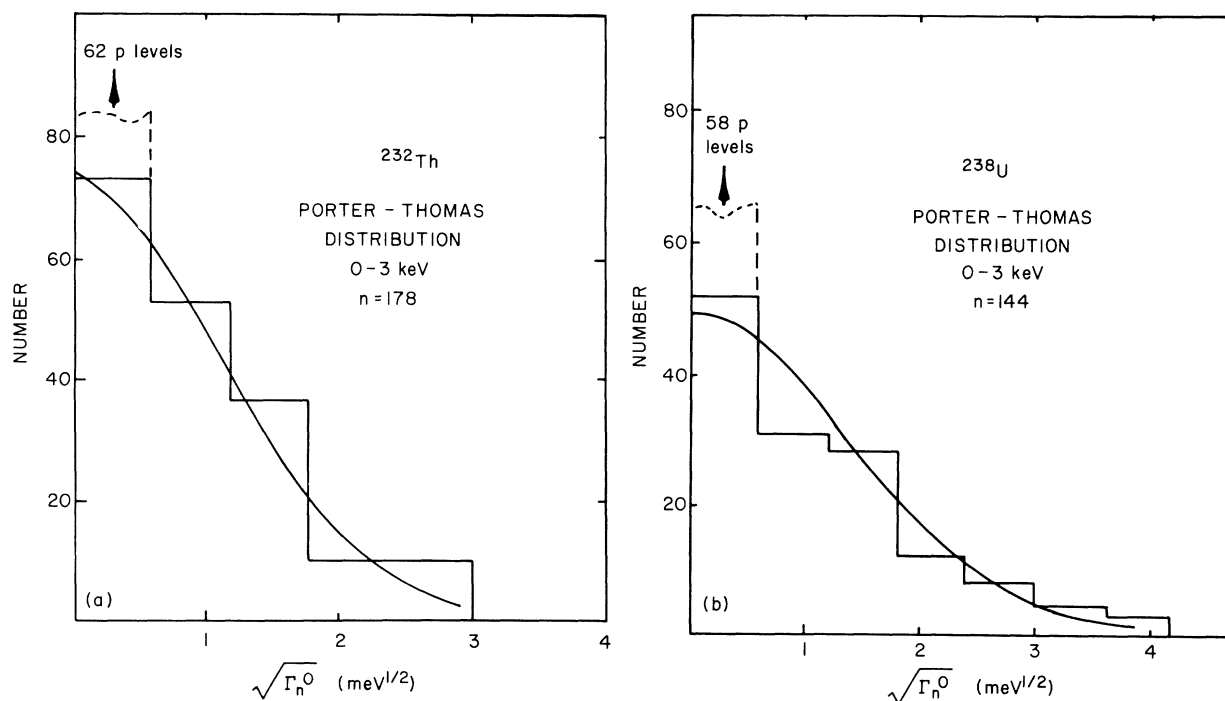


FIG. 9. (a), (b) The histograms for ^{232}Th and ^{238}U of the observed distributions of $(\Gamma_n^0)^{1/2}$ for levels which we selected as s wave in the energy region 0–3 keV. The curves have been normalized to the s -wave strength functions. There is excellent agreement between the theoretical P.T. curves ($\nu = 1$) and the experimental data.

(b) the fractional uncertainties in these $g\Gamma_n^1$ values are relatively large; and (c) these weak levels are mainly seen using the thickest samples, where a significant fraction of the energy range is not satisfactory for observing weak p levels due to the effects of the strong s levels; and (d) an inspection of the N versus E plots for all levels, Fig. 7, shows that there is a greatly reduced detection efficiency for p levels above ~ 400 eV for ^{232}Th , and ~ 1200 eV for ^{238}U . One method used is to assume that the true p -level density is three times that of s levels (due to statistical factors) and that $\langle g\Gamma_n^1 \rangle$ is the same for $p_{1/2}$ and $p_{3/2}$ levels, so the true $g\Gamma_n^1$ distribution is given by the P.T. theory. Various boundary $(g\Gamma_n^1)_A$ values are chosen such that most p levels, which are not too close to strong s levels, will be detected if $(g\Gamma_n^1) \geq (g\Gamma_n^1)_A$. An estimate is then made of the effective energy interval, ΔE_1 , available away from the strong s levels in the full region ΔE . One can then determine the true $\langle g\Gamma_n^1 \rangle$ which would give, on average, the observed number of levels $\geq (g\Gamma_n^1)_A$ in ΔE_1 . Such an analysis gives $10^4 S_1 \sim 0.9$ for the 12 p levels in ^{232}Th to 402.6 eV having $g\Gamma_n^1 \geq 2.5$ meV, using $\Delta E_1 \sim 0.8\Delta E$. For $10^4 S_1 = 0.6$ and 1.4, we would have expected to have, on average, 7.2 or 18.4 levels with $g\Gamma_n^1 \geq 2.5$ meV, respectively. These are the rough limits on our estimate of S_1 for ^{232}Th . There are 10 levels in ^{238}U to 1200 eV having $g\Gamma_n^1 \geq 10$ meV. For an effective $\Delta E_1 \sim 0.8\Delta E$ in this interval, and an expected 148 p levels per keV, a value of $\langle g\Gamma_n^1 \rangle = 2.95$ meV is required, with $10^4 S_1 = 1.43$. Values of $10^4 S_1 = 1.73$ and 1.16 would yield 14 and 6 mean numbers of p levels having $g\Gamma_n^1 > 10$ meV in this interval. These values are the approximate upper and lower bounds for our evaluation. These

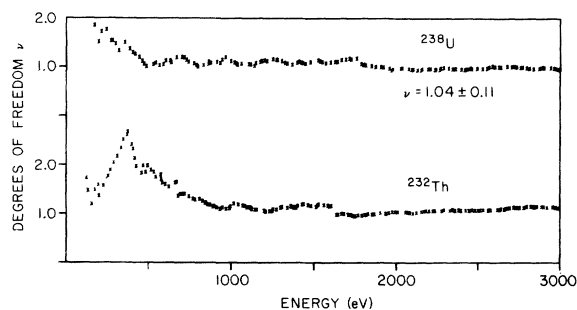


FIG. 10. Results of χ^2 analysis to determine the "effective number of degrees of freedom," ν , for our observed distributions of $g\Gamma_n^1$ values for ^{232}Th and ^{238}U for our selected s level populations. The large fluctuation in ν for ^{232}Th below 500 eV has been emphasized in the literature and remains unexplained, since it has a very low probability of occurrence according to the P.T. theory, in the absence of fluctuations in the intrinsic S_0 . The experimental values for the full energy interval are consistent with the single-channel value $\nu = 1$.

results clearly depend on the choice to which levels are s and which are p . Our own selection logic is discussed in Ref. 9.

The above evaluation of S_1 may be compared with experiments in other laboratories. Ribon (Saclay)¹⁰ observed many more weak levels in ^{232}Th than we find. He obtains $10^4 S_1 = 1.55$ for E up to 500 eV, and gives a "best choice" of $10^4 S_1 =$

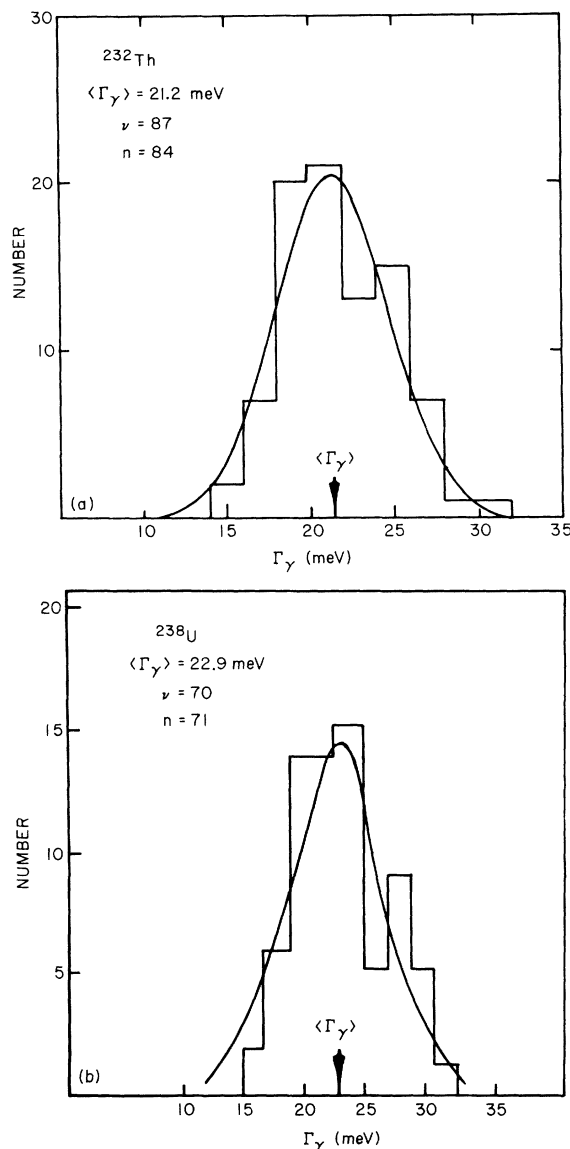


FIG. 11. (a), (b) Distribution of the total radiation widths, Γ_γ , obtained from the analysis of ^{232}Th and ^{238}U . The data have been fitted with χ^2 curves of 87 and 70 degrees of freedom, respectively. These ν values should be considered to be the lower limit on the true number of degrees of freedom. The divergence of the individual Γ_γ values from the mean is thought to be due mainly to experimental uncertainties.

$= (1.4 \pm 0.5)$. However, since he distinguished s and p levels by means of bands of $g\Gamma_n$ values, and the P.T. distribution mixes weak s and strong p levels, we have reexamined his analysis, deleting from his p -level population those levels which we consider to be s levels. This removes three of the stronger levels from his p population in the 0–500-eV region. A similar analysis as above gives 14 observed p levels having $g\Gamma_n^1 \geq 2.5$ meV to 400 eV, where we have 12 levels. His revised S_1 is then a little bigger than ours, but well within our quoted limits. The other main evaluation of p levels is due to Forman *et al.*¹⁵ (LASL) from an experiment using a nuclear explosion. They tend to have larger $g\Gamma_n^1$ than ours for weak levels that we also observe. Some levels that we see, they were unable to observe due to strong nearby resonances. They quote a value of $\langle g\Gamma_n^1 \rangle = 3.9$ meV. For their $\langle D \rangle = 7.5$ eV for p levels, which is higher than our value of 5.6 eV, they get $10^4 S_1 = 1.7$. A reexamination of their $g\Gamma_n^1$ values for levels which we do not call s levels gives 10 levels to 402 eV having $g\Gamma_n^1 \geq 2.5$ meV versus our 12 levels. This would give a value of S_1 consistent with, but slightly lower, than ours for that region. Other evaluations of S_1 for ^{232}Th using $\langle \sigma_t \rangle$ versus E in the higher energy region of unresolved resonances give $10^4 S_1 = 1.64 \pm 0.24$ (Harwell¹⁸) and 2.1 (Duke¹⁷).

For ^{238}U the comparisons of $10^4 S_1$ from other laboratories are as follows. Bollinger and Thomas¹⁹ obtain $(2.14_{-1.0}^{+2.0})$ for p levels below about 170 eV. The atomic bomb results of Glass *et al.*¹⁶ give (1.8 ± 0.3) to 800 eV. Correcting for contributions from levels which we treat as s levels reduces this to 1.6. Divadeenam¹⁷ (Duke) obtained 1.9 from $\langle \sigma_t \rangle$ versus E behavior, and Uttley, Newstead, and Diment¹⁸ (Harwell) obtained $(2.44_{-0.28}^{+0.16})$ from a similar technique. We are not prepared to comment on the over-all uncertainties of experimental strength function determinations using average total cross sections.

The average capture width $\langle \Gamma_\gamma \rangle$ in ^{232}Th for the 84 levels to 2.4 keV from Table I was $[21.2 \pm 0.3(\text{stat.}) \pm 0.9(\text{syst.})]$ meV. We have estimated a systematic uncertainty of 0.9 meV due to the determination of the “saturated open” of the neutron beam in the self-indication results. This value compares with $\langle \Gamma_\gamma \rangle = (20.5 \pm 3)$ meV obtained by Forman *et al.*,¹⁵ and 20.9 and 21.6 meV obtained by Asghar *et al.*¹¹ and Ribon,¹⁰ respectively. As expected all of our individual Γ_γ values lie close to the mean of 21.2 meV, with few values more than 20% away from the average. This is consistent with a large number of possible γ -ray transitions between initial and final states from the $\frac{1}{2}^+$ capture state. The usual P.T. χ^2 analysis gives:

$$\frac{2}{\nu} = [\langle \Gamma_{\gamma i}^2 \rangle - \langle \Gamma_{\gamma i} \rangle^2] / \langle \Gamma_{\gamma i} \rangle^2$$

which is the fractional mean squared spread in the values. This gives $\nu = 87$ for ^{232}Th . The distribution of $\Gamma_{\gamma i}$ values is shown in Fig. 11(a). Most of the above spread in the $\Gamma_{\gamma i}$ values probably comes from experimental errors in the measured values, so that the true ν is probably very much larger. Another feature of the algebraic P.T. analysis is the implicit assumption that the various $\langle \Gamma_{\gamma j} \rangle$ are the same for different j . This is certainly incorrect because of spectroscopic factors and transition energy dependencies. When $\langle \Gamma_{\gamma j} \rangle$ values have a large variation for different j , the stronger transitions dominate in determining the spread in the true $\Gamma_{\gamma i}$ values, which is then for a much smaller effective number of degrees of freedom than the true number of capture channels. For these experimental and theoretical reasons our value of ν is a lower limit and the true value of ν is probably very much larger.

For ^{238}U , our average capture width for the 71 levels in Table III up to 2.4 keV is $\langle \Gamma_\gamma \rangle = [22.9 \pm 0.5(\text{stat.}) \pm 0.9(\text{syst.})]$ meV. This compares with values of $\langle \Gamma_\gamma \rangle$ reported by Rosen (I) (24.6 ± 0.8) , Asghar, Chaffey, and Moxon¹² (23.74 ± 1.09) , Rohr, Weigmann, and Winter¹³ (24.64 ± 0.85) , and Glass *et al.*¹⁶ (20.6 ± 1.7) . Figure 11(b) shows our experimental distribution of Γ_γ values, which are best fitted by a χ^2 distribution of 70 degrees of freedom. We did not observe what we would consider to be significant periodic or quasiperiodic fluctuation of the Γ_γ values versus energy in ^{238}U , as reported by Glass *et al.*, whose values were more widely distributed about their $\langle \Gamma_\gamma \rangle$. This conclusion is in agreement with the recent work of Malecki *et al.*²⁰ (Dubna) who likewise do not find a divergence of the separate radiation widths from the average exceeding the measurement error, and who obtain $\langle \Gamma_\gamma \rangle \sim 24$ meV. Their 31 values of Γ_γ for individual levels are all between 22 and 27 meV.

V. SUMMARY AND CONCLUSIONS

The high-resolution measurements obtained during our 1970 experimental series allowed us for the first time to obtain results for the essentially complete s -level population in the energy region 0 to 3 keV for the important reactor materials ^{232}Th and ^{238}U . The chosen value of S_0 for these isotopes was based on data to 4 keV. Our present values of S_0 are higher than our previous 1964 results which seem, in retrospect, to systematically underestimate the Γ_n^0 values for levels above 1 keV. Our new results are in agreement with other recent measurements. We found the P.T. distribution for the reduced widths in ^{232}Th to be consis-

tent with our data for the energy range to 3 keV, although some anomalies remain for $E < 500$ eV as mentioned by Ribon and by Forman *et al.* Furthermore, for ^{238}U , we were not able to reproduce the low value of $\langle \Gamma_\gamma \rangle = 19$ meV and the quasiperiodic fluctuations in the individual Γ_γ values reported by Glass *et al.* Our estimate of the p -wave strength functions are lower than those of most other authors using methods based on individual resonance parameters and $\langle \sigma_t \rangle$ versus E behavior. This is largely due to our selection procedure for the s population.

ACKNOWLEDGMENTS

We wish to thank Dr. G. Rogosa of the U. S. Atomic Energy Commission for his aid in obtaining our samples. John Arbo greatly contributed in the data taking and calibration parts of the M-R measurements. We gratefully acknowledge the assistance of the other members of the group including Dr. C. Ho, Dr. W. Makofske, C. Gilman, W. Marshall, and D. Liang.

†Research supported by the U. S. Atomic Energy Commission.

*Present address: National Bureau of Standards, Gaithersburg, Maryland.

‡Present address: University of Cape Town, Cape Town, Union of South Africa.

¹Earlier papers in this series: I: J. Rosen, J. S. Desjardins, J. Rainwater, and W. W. Havens, Jr., *Phys. Rev.* **118**, 687 (1960), ^{238}U ; II: J. S. Desjardins, J. L. Rosen, W. W. Havens, Jr., and J. Rainwater, *ibid.* **120**, 2214 (1960), Ag, Au, Ta; III: J. B. Garg, J. Rainwater, J. S. Petersen, and W. W. Havens, Jr., *ibid.* **134**, B985 (1964), ^{232}Th , ^{238}U ; IV: J. B. Garg, W. W. Havens, Jr., and J. Rainwater, *ibid.* **136**, B177 (1964), As, Br; V: J. B. Garg, J. Rainwater, and W. W. Havens, Jr., *ibid.* **137**, B547 (1965), Nb, Ag, I, Cs; VI: S. Wynchank, J. B. Garg, W. W. Havens, Jr., and J. Rainwater, *ibid.* **166**, 1234 (1968), Mo, Sb, Te, Pr; VII: J. B. Garg, J. Rainwater, and W. W. Havens, Jr., *Phys. Rev. C* **3**, 2447 (1971), Ti, Ni, Fe; VIII: H. I. Liou, H. S. Camarda, S. Wynchank, M. Slagowitz, G. Hacken, F. Rahn, and J. Rainwater, *ibid.* **C 5**, 974 (1972), Er; IX: F. Rahn, H. S. Camarda, G. Hacken, W. W. Havens, Jr., H. I. Liou, J. Rainwater, M. Slagowitz, and S. Wynchank, *ibid.* **C 6**, 251 (1972), Sm, Eu. These papers are referred to by Roman numeral in the text.

²F. Rahn *et al.*, *Trans. Am. Nucl. Soc.* **14**, 805 (1971).

³F. Rahn *et al.*, in *Proceedings of the Third Conference on Neutron Cross Sections and Technology, Knoxville, Tennessee, 15 March 1971* (National Technical Information Service, U. S. Dept. of Commerce, Springfield, Virginia, 1971), Vol. II, p. 658.

⁴M. King Hubert, in *Resources and Man* (W. H. Freeman and Co., San Francisco, 1969).

⁵H. Hummel, in *Proceedings of the Third Conference on Neutron Cross Sections and Technology, Knoxville, Tennessee, 15 March 1971* (see Ref. 3), Vol. I, p. 65.

⁶F. J. Dyson, *J. Math. Phys.* **3**, 140, 157, 166, 1199 (1962).

⁷M. L. Mehta and F. J. Dyson, *J. Math. Phys.* **4**, 701, 713 (1963).

⁸A. Prince, in *Proceedings of the Conference on Nu-*

clear Data for Reactors, Helsinki, 15 June 1970 (International Atomic Energy Agency, Vienna, Austria, 1970), Vol. II, p. 825.

⁹H. I. Liou, H. S. Camarda, and F. J. Rahn, *Phys. Rev. C* **5**, 1002 (1972).

¹⁰P. Ribon, Ph.D. thesis, Université de Paris, 1969 (unpublished).

¹¹M. Asghar, C. M. Chaffey, M. C. Moxon, N. J. Patten- den, E. R. Rae, and C. A. Uttley, *Nucl. Phys.* **76**, 196 (1966).

¹²M. Asghar, C. M. Chaffey, and M. C. Moxon, *Nucl. Phys.* **76**, 305 (1966).

¹³G. Rohr, H. Weigmann, and J. Winter, in *Proceedings of the Conference on Nuclear Data for Reactors, Helsinki, 15 June 1970* (see Ref. 8), Vol. I, p. 413.

¹⁴G. Carraro and W. Kolar, in *Proceedings of the Third Conference on Neutron Cross Section and Technology, Knoxville, Tennessee, 15 March 1971* (see Ref. 3), Vol. II, p. 701.

¹⁵L. Forman, A. D. Schelberg, J. H. Warren, M. V. Harlow, H. A. Grench, and N. W. Glass, in *Proceedings of the Third Conference on Neutron Cross Sections and Technology, Knoxville, Tennessee, 15 March 1971* (see Ref. 3), Vol. II, p. 735.

¹⁶N. W. Glass, A. D. Schelberg, L. D. Tatro, and J. H. Warren, in *Proceedings of the Second Conference on Neutron Cross Sections and Technology, Washington, D. C., 4 March 1968* (U. S. G.P.O., National Bureau of Standards Special Publication No. 299, 1968), Vol. I, p. 573.

¹⁷M. Divadeenam, Ph.D. thesis, Duke University, 1968 (unpublished).

¹⁸C. A. Uttley, C. Newstead, and K. Diment, in *Proceedings of the Conference on Nuclear Data, Microscopic Cross Sections and Other Data Basic for Reactors, Paris, 1961* (International Atomic Energy Agency, Vienna, Austria, 1967), Vol. I, p. 165.

¹⁹L. Bollinger and G. Thomas, *Phys. Rev.* **171**, 1293 (1968).

²⁰H. Malecki, L. B. Pikel'ner, M. Salamatin, and E. I. Sharapov, *At. Energ. (USSR)* **32**, 49 (1972) [transl.: *Soviet J. At. Energy* **32**, 45 (1972)].